Solar Activity and its Magnetic Origin
Proceedings IAU Symposium No. 233, 2006
V. Bothmer & A. A. Hady, eds.

doi:10.1017/S1743921306001359

Magnetic flux emergence into the atmosphere

F. Moreno-Insertis[1,2]

[1]Instituto de Astrofisica de Canarias, 38200 La Laguna (Tenerife), Spain
email: fmi@ll.iac.es

[2]Dept of Astrophysics, Univ of La Laguna, Tenerife, Spain

Abstract. Understanding the mechanism that causes the emergence of magnetic flux from the solar interior to the atmosphere, the drastic changes in the properties of the matter and magnetic fields along the rise and the interplay of dynamic and resistive phenomena that shape the emerged regions is one of the major open tasks in solar physics. Important advances are being made both in the theoretical modelling and in the observation of the emergence events. This review concentrates on recent advances through 3D numerical experiments carried out with massively parallel MHD and radiative transfer codes.

Keywords. Sun:activity, Sun: magnetic fields, Sun:corona, Sun:photosphere, methods: numerical, plasmas, MHD, radiative transfer

1. Introduction

The solar atmosphere is being continually stirred by the eruption of magnetized plasma from below the photosphere. Magnetic flux emergence takes place on a large variety of space and time scales: the observed range stretches from very small magnetic elements emerging in the interior of supergranular cells to the giant eruptions that produce large active regions, often associated with the emission of coronal mass ejections. There are still many fundamental open questions concerning the emergence of flux into the solar atmosphere. Yet, a new set of observational facilities from space (e.g., the Solar B, SDO and Stereo satellites, with launch dates between 2006 and 2008) and on the ground (like the SST, DOT and Gregor telescopes, in the Observatories in the Canary Islands) permit to observe the emergence episodes with unprecedented space and time resolution. This fact, combined with the fast increase in computational power, promises an era of substantial advances in our knowledge of the events taking place during magnetic flux emergence and of the physics behind them.

Theoretical modelling of the process of magnetic flux emergence is fraught with large difficulties: magnetized plasma emerging through the photosphere and chromosphere into the corona traverses no less than 10 pressure scaleheights, whereby it goes from a high-β to a low-β regime; it is optically thick in the interior and ends up being transparent to electromagnetic radiation in the corona; its temperature decreases in the low atmosphere through radiative cooling and expansion but reaches high values once the emerged plasma is in the corona, where it becomes observable in the EUV and in X-rays. The magnetic and viscous Reynolds numbers of the system are extremely high, implying that diffusive processes (including reconnection) will take place over very small spatial scales, impossible to resolve either observationally or in computer models.

As a result of the difficulties just explained, advances in theoretical understanding have been comparatively slow in the past decades. The early numerical experimentation effort focused on two-dimensional configurations (e.g., Shibata *et al.* 1989, 1992; Nozawa

et al. 1992; Yokoyama & Shibata 1995, 1996). These models were particularly successful at explaining the formation of plasmoids and the ejection of hot, fas jets, like those measured in X-rays by the Yohkoh satellite (see Shimojo *et al.* 1996), as a by-product of the reconnection process taking place at the interface between emerging magnetized plasma and a pre-existing coronal magnetic field (Yokoyama & Shibata 1994, 1995, 1996).

Two-dimensional models are good starting points to understand the physics of flux emergence events. However, emerging magnetic elements and regions in the Sun show no 2D symmetry: the problem of flux emergence is intrinsically three-dimensional. A few early 3D models were calculated in the 1990's (Matsumoto & Shibata 1992; Matsumoto *et al.* 1993, 1998), even though, naturally, with limited computational means. The current decade is witnessing an impressive upsurge in the number of 3D flux emergence experiments and the variety of aspects covered by them (e.g., Fan 2001; Magara & Longcope 2001, 2003; Abbett & Fisher 2003; Fan & Gibson 2003, 2004, 2006; Archontis *et al.* 2004, 2005, 2006; Magara 2004; Manchester *et al.* 2004; Galsgaard *et al.* 2005; Isobe *et al.* 2005; Cheung *et al.* 2006). In what follows, I will review some of the results obtained in those experiments, paying special attention to the differences between models with or without a detailed treatment of the radiative transfer in the low atmosphere (Sec. 2). In Sec. 3, I will briefly comment on the formation of current sheets ensuing upon the collision of an emerging and a preexisting magnetic system (Sec. 3.1) and the 3D nature of the reconnection in them (Sec. 3.2). Further aspects of the physics of flux emergence studied through recent 3D models have been reviewed by Moreno-Insertis (2006a,b).

2. Emerging regions at the photosphere

2.1. *Models with strongly simplified thermodynamics*

Most of the modelling activity in this field has left aside the complicated physics associated with radiative phenomena in the atmosphere. This can be reasonable as a first step: considering the interaction between the radiation field and the plasma involves solving the equation of transfer for the radiation field in different wavelength bands and along rays in different directions, turning the problem from three-dimensional to six-dimensional (even though the three additional dimensions are sampled with a low number of points in most radiation-hydrodynamics models). The problem becomes even more demanding if non-LTE effects are studied, which are of particular importance in the chromosphere. Including radiation aspects so far has been too expensive from a computational point of view for the models with spatial domain stretching from the top of the solar interior to the corona. In those cases, the authors have ignored the interaction with radiation; the entropy of the plasma, therefore, varies only through (explicit or numerical) viscous and ohmic dissipation and, in some cases, through thermal conduction effects.

Such models do not attempt to match in detail the observed distributions of temperature, velocity or magnetic field in those regions where radiative effects are important, particularly in the photosphere, where strong radiative cooling takes place on short timescales compared with the emergence timescales. They, correspondingly, concentrate for the most part on the coronal stages of the rise, focusing, in particular, on the interaction with preexisting coronal magnetic fields (Sec. 3). for the sake of simplicity, also, the initial stratification typically consists of two isothermal domains, with temperature ratio between them of, e.g., 200, mimicking the photosphere and corona; those domains are joined by a region with a steep temperature gradient, as a sort of transition region; the whole domain above the photosphere typically extends for some 10 Mm. A domain with adiabatic (in some cases, slightly superadiabatic) stratification is appended below

https://doi.org/10.1017/S1743921306001359 Published online by Cambridge University Press

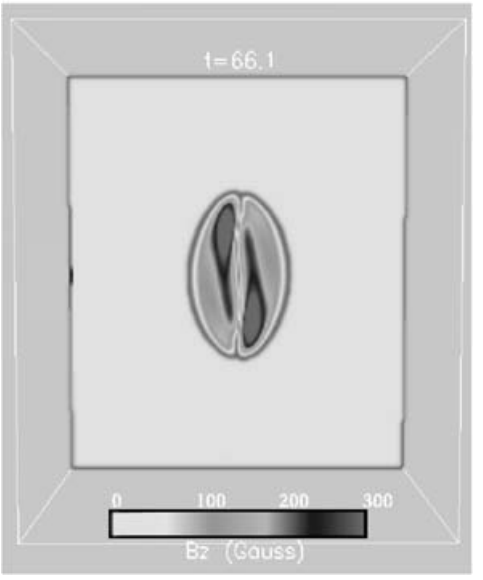

Figure 1. Map of the unsigned flux density at the photosphere constructed with the data of the experiment of Archontis *et al.* (2004). The emergence process is at an intermediate stage and shows the *tadpole*- or *tongue*-shape adopted by the opposite polarities.

the photosphere reaching down to a maximum of a few Mm inside the Sun. A horizontal magnetic structure (typically a twisted flux tube; in some models a magnetized horizontal sheet) is planted toward the bottom of the stratification, and the gas pressure in the magnetized plasma is adjusted so that there is continuity of the total stress tensor (gas + magnetic). To start the dynamical evolution, different methods are used: for magnetic tubes, in most cases a non-homogeneous density distribution is given to the tube, so that the central part is buoyant and rises, yielding a classical Ω-loop (Fan 2001; Archontis *et al.* 2004, 2005, 2006; Manchester *et al.* 2004; Galsgaard *et al.* 2005). Alternatively, an upward-directed velocity field is imposed to the central part of the tube in the initial stages of the evolution that brings it out of its initial configuration until the central part is sufficiently buoyant for it to continue rising with no extra velocity field (Magara & Longcope 2001, 2003; Magara 2004). For magnetized sheets, the evolution is typically initiated self-consistently by letting a magnetic buoyancy instability develop at the interface between magnetized and unmagnetized plasma, which yields a magnetic arch system that rises to the corona (Matsumoto *et al.* 1993, 1998; Isobe *et al.* 2005).

In spite of the strongly simplified thermodynamics, the models show qualitative agreement with a number of features observed in emerging active regions at the photosphere. An example is the *tadpole* or *tongue-like* shape of the magnetic polarities in the active region that have been shown by Fan (2001), Magara & Longcope (2001) and Archontis *et al.* (2004) to result naturally from the emergence of a twisted magnetic tube (Fig. 1). Assume a buoyant magnetic tube initially with its axis along the East-West direction. If the field lines are sufficiently twisted, the first layers reaching the photosphere will show a comparatively weak magnetic field oriented in the North-South direction. However, the rising tube has an Ω-shape, so that, after further emergence, a bipolar structure will become clearly discernible determined by the cut of a horizontal plane with the flanks of the rising loop. Hence, one expects to obtain a shape as shown in Fig. 1: the vertical axis of the figure coincides with the East-West direction: two concentrated polarities are

https://doi.org/10.1017/S1743921306001359 Published online by Cambridge University Press

visible, followed by a *tongue* of weaker field stretching toward the other polarity, surrounded by regions of still weaker field strength. Structures of this type have been repeatedly observed in emerging active regions (see, e.g., Strous *et al.* 1996; López Fuentes *et al.* 2000). Additionally, in the models, the velocity field at the photosphere shows a strong shear on either side of the line dividing the two polarities (central vertical axis in Fig. 1). This is due to the sign and direction of the horizontal component of the Lorentz force at that height (Fan 2001). Again, this feature has been observed in the early stages of the formation of active regions (Strous *et al.* 1996). Finally, the field strength for the photospheric features formed in these experiments is not far from the values obtained in photospheric observations. In fact, in this class of numerical experiments with magnetic regions rising to the corona, the field strength at the photosphere cannot be much lower than observed in emerging active regions: the further rise into the corona is possible in spite of the subadiabatic stratification of the photosphere through the development of a magnetic buoyant instability. For the instability to develop, the plasma β must be below a threshold (see Moreno-Insertis 2006a); that threshold corresponds to field strength values not far from those observed. In any case, any results concerning instabilites at the photosphere must be taken with care: the field strength at the photosphere in the Sun is strongly affected by radiative phenomena, which are not included in the models discussed in this section.

2.2. *Models with detailed radiative transfer*

Flux emergence modelling including detailed photospheric radiative transfer (RT) has been recently carried out by Cheung *et al.* (2006; see also Cheung 2006). The height range used in these models is necessarily much more limited than that of the models of the previous section and includes from close to 2 Mm below the photosphere to about 500 km above it: no chromosphere or corona is included in the calculation. The calculation is done using the MHD + RT code of Vögler *et al.* (2005). Concerning the RT part, in particular, radiation scattering is neglected, local thermodynamic equilibrium is assumed for the source function and the *frequency binning* method is used to deal with the opacities; the latter method in effect discretizes the frequency axis; in the models by Cheung (2006) either one or four frequency bins were used. These simplifications, together with the use of 3 ray directions per quadrant, render the calculation affordable in spite of the large computational demands of radiation hydrodynamics calculations.

The experiment of Cheung *et al.* (2006) first lets granular convection reach a statistically stationary state with no magnetic field. The convection has broad upflows and concentrated downflows, which become thin toward deep levels, as is common in realistic convection simulations (e.g., Stein & Nordlund 1998; Vögler *et al.* 2005). A magnetic tube is then planted close to the bottom of the convecting region and time is reset to $t = 0$. Two cases are considered: in the first one, the tube is given a comparatively weak initial field strength of 2500 G at the axis (local plasma β of 22) and a total longitudinal magnetic flux of $3\,10^{18}$ mx. The entropy in the magnetized domain is made uniform and equal to the average of the upflowing regions at that height before the tube was introduced; the tube is, therefore, buoyant and tends to rise. However, the field intensity is not high enough for the tube to rise in the downflows. This can be seen by estimating the terminal velocity of a thin tube in a downflow given by the equilibrium between buoyancy force and aerodynamic drag (e.g., Moreno-Insertis 1983; Emonet & Moreno-Insertis 1998; Cheung 2006). As shown in the latter work, 2500 G at the axis provides too low a buoyancy force to withstand the drag of the downflows. More in general, the magnetic field in that tube cannot withstand the disrupting effect of the convective flows: the magnetized plasma is passively advected and the magnetic flux emerging in the photosphere has no

https://doi.org/10.1017/S1743921306001359 Published online by Cambridge University Press

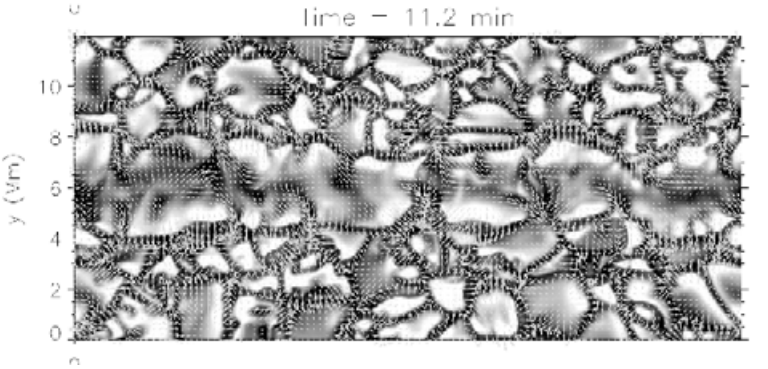

Figure 2. Continuum intensity map at 5000 Å showing granular cells with the horizontal velocity field superimposed as arrows. Morphologically different granules and a dark lane can be seen in the horizontal band where the magnetic flux tube is emerging. (From Cheung 2006).

coherent tube-like appearance; rather, it consists of a mixture of interspersed polarities of opposite sign.

In the second case, a stronger field intensity, 8500 G, was given at $t = 0$, yielding a total longitudinal magnetic flux of 10^{19} mx. In this case the initial field strength is above the value where drag and buoyancy would compensate each other in the downflows. Hence, the tube rises both in the up- and downflows. However, the field strength is not strong enough to prevent the distortion of the tube by the convection flows along the rise. When the tube emerges, the granulation pattern becomes modified by the presence of the magnetic field (see Fig. 2). The velocity arrows also show a coherent sideways expansion associated with the rising tube. Through a set of experiments with modified initial conditions, Cheung (2006) has also been able to reproduce the development of a small (ephemeral) active region.

3. The rise into the upper atmosphere: collision of magnetized domains

One of the most interesting aspects of the models that study the rise of magnetic flux from the interior to the corona is that they show directly the drastic change of physical properties (density, pressure, plasma beta) undergone by the rising plasma and the links that become established between the dense photosphere and the tenous corona. In particular, when the corona has a magnetic field distribution prior to the emergence of new flux, the upcoming and preexisting magnetic systems collide, a concentrated current sheet is formed at their interface, and reconnection between the field lines of the two systems ensues. In the general, non-symmetric cases studied in the recent 3D models, the shape and structure of the current sheet and reconnection itself are fully three-dimensional: the useful, simplified 2D models that have guided the physical intuition for many years are insufficient to explain the events observed. In this section we summarize a number of properties of the current sheet and explain various features that clearly show intrinsincally three-dimensional aspects of the reconnection process.

3.1. *Formation of current sheets*

We consider here the current sheet formed when a buoyant magnetic tube initially located below the photosphere breaks through the surface and, upon further rise across the low atmosphere, impinges on a preexisting simple, horizontal and uniform magnetic field in

https://doi.org/10.1017/S1743921306001359 Published online by Cambridge University Press

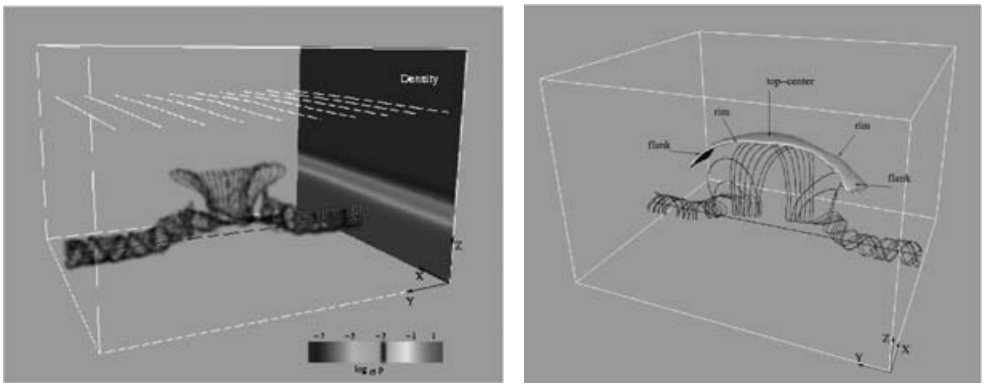

Figure 3. Left: twisted flux rope with the central part rising toward the corona. A layer of the preexisting coronal magnetic field is also shown. Right: arch– or ribbon–like current sheet formed upon contact of the two systems: the solid surface is an isosurface of the current intensity, with tags attached to some of its geometrical elements. From Archontis *et al.* (2005).

the corona. This case has been describe in detail by Archontis *et al.* (2005) (see also Galsgaard *et al.* 2005 and Archontis *et al.* 2004, 2006). These experiments belong to the class with no detailed radiative transfer discussed above. Fig. 3 presents an illustration of the process of formation of the current sheet. The left panel shows the field line configuration in the central part of the rising tube shortly before the collision with the coronal field takes place: the large expansion associated with the rise leads to a fan–shape of the field lines in the central segments of the tube. On the right panel, collision has occurred and a current sheet (indicated by an isosurface of the current intensity) has formed. In fact, the current sheeet covers the upcoming plasma as a sort of cap; however, the current intensity is concentrated toward the apex and flanks of the rising system, so the sheet adopts the shape of a *bridge* or *ribbon* visible in the figure. The case of Fig. 3 was particularly simple in that the field in the two colliding systems was almost antiparallel at the time of collision. A more general configuration, with angle betwen the fields in the colliding systems different from 180 deg (but still providing for a substantial field jump) yields a current *ribbon* no longer parallel to the axis of the rising tube (Galsgaard *et al.* 2005).

The properties of this current sheet are very different from those of simple stationary 2D models: density, velocity, and magnetic field strength are generally quite different on the sides of the sheet and the evolution is non-stationary. Magnetized plasma is fed from both sides toward the current sheet, where the field lines reconnect. Once inside the sheet, the plasma is heated through ohmic dissipation. The density of the material coming into the sheet steadily decreases as the interface between the two systems rises in the atmosphere. The consequence is that the plasma inside the current sheet goes from dense and (comparatively) cool plasma to having ρ and T with typical coronal values. Plasmoids are generated within the sheet, probably as a consequence of the tearing mode instability (Archontis *et al.* 2006; see also Isobe *et al.* 2005); these 3D plasmoids are no magnetic islands: they have the shape of solenoids contained within the current sheet with individual field lines being linked to the external magnetic system at the end of the solenoid. The windings of the solenoid are more or less tightly wound depending on the mutual orientation of the field systems on the sides of the current sheet. The plasmoids get expelled from the current sheet through a classical melon-seed mechanism.

https://doi.org/10.1017/S1743921306001359 Published online by Cambridge University Press

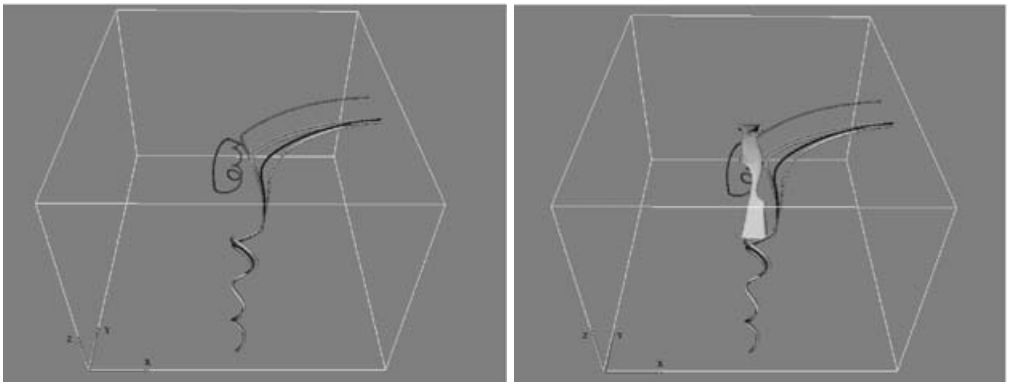

Figure 4. Continuous reconnection of a field line of the magnetic tube with field lines of the preexisting coronal field. A single field line in the tube (front of the figure) reconnects successively with different field lines in the corona (visible as asymptotically horizontal lines going to the right hand side of the box). The two panels are identical, except for the current isosurface on the right panel, which shows the extent of the diffusion region. From Archontis *et al.* (2005).

3.2. *Continuous reconnection*

The field lines brought from either side to the current sheet undergo reconnection: there result magnetic lines that link the corona to the photospheric and subphotospheric magnetic field system. Reconnection is generally assumed to occur as a single, instantaneous event for each field line: two separate field lines are brought to the diffusion region where, at a given instant, they are cut and joined to each other. In a three-dimensional situation this needs not be the case: as explained by Priest *et al.* (2003a,b), when the reconnecting field lines are not all contained in a single plane (which is the general situation in three dimensions), the reconnection may not take place as a one-off process; rather, the field lines change connectivity continuously while they are within the diffusion region. Archontis *et al.* (2005) have found clear evidence of this continous change of connectivity. They consider (Fig. 4) a field line in the part of the tube buried below the photosphere (left panel, front part of the box). Following the windings of that field line along the tube into the box, at some point it becomes strongly inclined, crosses the photosphere and goes into the emerged part of the rising plasma system. Following that field line further on toward the back of the box, it dives down again and ends up in the subphotospheric part of the tube (final winding close to the back of the box). At a slightly later time, however, the field line has reconnected. The buried part at the front has barely moved; yet, the emerged part has changed connectivity, and now it abruptly changes direction and turns to the right, cutting the right-hand side vertical boundary of the box. In 2D, the new connectivity would be kept for all later times. In the 3D case, however, tracing the field line at successive times, we see the successive field lines shown in the left panel turn abruptly to the right boundary of the box with end point increasingly closer to the front of the figure. These, however, are not field lines frozen to the plasma: by calculating the velocity of the end point of the field line in the box, one concludes that it is much higher than the local plasma speed: the velocity of the end points is not a material velocity, but rather follows from the fact that the field lines are changing connectivity for as long as they are within the diffusion region. The end points eventually adopt the velocity of the local plasma when the whole field line has come out of the diffusion region: this can be seen through the right panel, which shows the same field lines but now also includes the current sheet where the reconnection is taking place.

https://doi.org/10.1017/S1743921306001359 Published online by Cambridge University Press

4. Outlook

Large three-dimensional MHD numerical experiments with extended grids (say upward of 512^3 grid points) and including the solution of the radiation transfer equation are within reach by using the largest computers available for research in the world. In the coming years they will allow to solve the combined MHD-RT flux emergence problem with domain extending from several Mm in the interior to the corona. Together with the excellent observational possibilities that are becoming available at present, they are likely to lead to rapid advances in the understanding of the difficult but fascinating physics behind flux emergence events.

References

Abbett, W. P. & Fisher, G. H. 2003, *ApJ*, 582, 475
Archontis, V., Galsgaard, K., Moreno-Insertis, F., & Hood, A. 2006, *ApJ Lett*, 645, L161
Archontis, V., Moreno-Insertis, F., Galsgaard, K., & Hood, A. 2005, *ApJ*, 635, 1269
Archontis, V., Moreno-Insertis, F., Galsgaard, K., Hood, A., & O'Shea, E. 2004, *A&A*, 426, 1047
Cheung, M. C. M. 2006, PhD Thesis (Univ. Göttingen)
Cheung, M. C. M., Schüssler, M., & Moreno-Insertis, F. 2006, *ApJ*, in preparation
Emonet, T. & Moreno-Insertis, F. 1998, *ApJ*, 492, 804
Fan, Y. 2001, *ApJ*, 554, L111
Fan, Y. & Gibson, S. E. 2003, *ApJ*, 589, L105
—. 2004, *ApJ*, 609, 1123
—. 2006, *ApJ*, 641, L149
Galsgaard, K., Moreno-Insertis, F., Archontis, V., & Hood, A. 2005, *ApJ*, 618, 153
Isobe, H., Miyagoshi, T., Shibata, K., & Yokoyama, T. 2005, Nature, 434, 478
López Fuentes, M., Demoulin, P., Mandrini, C. H., & vanDriel Gesztelyi, L. 2000, *ApJ*, 544, 540
Magara, T. 2004, *ApJ*, 605, 480
Magara, T. & Longcope, D. W. 2001, *ApJ*, 559, L55
—. 2003, *ApJ*, 586, 630
Manchester, W., Gombosi, T., DeZeeuw, D., & Fan, Y. 2004, *ApJ*, 610, 588
Matsumoto, R. & Shibata, K. 1992, *Publ Astron Soc Japan*, 44, 167
Matsumoto, R., Tajima, T., Chou, W., Okubo, A., & Shibata, K. 1998, *ApJ*, 493, L43
Matsumoto, R., Tajima, T., Shibata, K., & Kaisig, M. 1993, *ApJ*, 414, 357
Moreno-Insertis, F. 1983, *A&A*, 122, 241
Moreno-Insertis, F. 2006a, in Solar MHD: Theory and Observations – a High Spatial Resolution Perspective, ed. J. Leibacher, H. Uitenbroek, & R. Stein, Astron Soc Pacific Conf Series
Moreno-Insertis, F. 2006b, in The 6th Solar-B Science Meeting, ed. K. Shibata, S. Nagata, & T. Sakurai, ASP Conference Series (San Francisco: Astronomical Society of the Pacific)
Nozawa, S., Shibata, K., Matsumoto, R., Sterling, A. C., Tajima, T., Uchida, Y., Ferrari, A., & Rosner, R. 1992, *ApJ Supl Ser*, 78, 267
Priest, E. R., Hornig, G., & Pontin, D. I. 2003a, *J Geophys Res*, 108, 1285
—. 2003b, Journal of Geophysical Research (Space Physics), 108, 6
Shibata, K., Nozawa, S., & Matsumoto, R. 1992, *Publ Astron Soc Japan*, 44, 256
Shibata, K., Tajima, T., Matsumoto, R., Horiuchi, T., Hanawa, T., Rosner, R., & Uchida, Y. 1989, *ApJ*, 338, 471
Shimojo, M., Hashimoto, S., Shibata, K., Hirayama, T., Hudson, H. S., & Acton, L. 1996, *Publ Astron Soc Japan*, 48, 123
Stein, R. F. & Nordlund, A. 1998, *ApJ*, 499, 914
Strous, L. H., Scharmer, G., Tarbell, T. D., Title, A. M., & Zwaan, C. 1996, *A&A*, 306, 947
Vögler, A., Shelyag,S., Schüssler, M., Cattaneo, F., Emonet, T., & Linde, T. 2005, *A&A*, 429, 335
Yokoyama, T. & Shibata, K. 1994, *ApJ Lett*, 436, 197
—. 1995, Nature, 375, 42
—. 1996, *Publ Astron Soc Japan*, 48, 353